American Journal of Pathology, Vol. 146, No. 1, January 1995

Animal Model

Onset and Progression of Pathological Lesions in Transforming Growth Factor-β1-Deficient Mice

Gregory P. Boivin,* Barbara A. O'Toole,* Ilona E. Orsmby,† Ronald J. Diebold,† Michael J. Eis,† Thomas Doetschman,† and Ann B. Kier‡

From the Division of Comparative Pathology, Departments of Pathology and Laboratory Medicine and Microbiology and Molecular Genetics,† University of Cincinnati College of Medicine, Cincinnati, Ohio, and Department of Pathobiology,‡ College of Veterinary Medicine, Texas A & M University, College Station, Texas*

Null-mutant (knockout) mice were obtained through disruption of the sixth exon of the endogenous transforming growth factor-β1 allele in murine embryonic stem cells via homologous recombination. Mice lacking transforming growth factor-β1 (mutants) were born grossly indistinguishable from wild-type littermates. With time, mutant mice exhibited a wasting phenotype that manifested itself in severe weight loss and dishevelled appearance (between 15 and 36 days of age). Examination of these moribund mice histologically revealed that transforming growth factor-β1-deficient mice exhibit a moderate to severe, multifocal, organ-dependent, mixed inflammatory cell response adversely affecting the heart, stomach, diaphragm, liver, lung, salivary gland, and pancreas. Because of the known multifunctional nature of transforming growth factor-β1 on the control of growth and differentiation of many different cell types, it is important to determine the degree to which the inflammatory response interacts with or masks other deficiencies that are present. To this end, we examined the extent and nature of the inflammatory lesions in different ages of neonatal knockout mice (5, 7, 10, and 14 days of age) and older moribund mice (>15 days of age) and compared them with the histology seen in wild-type normal animals. Mild inflammatory infiltrates were first observed in 5-day mutant mice in the heart, by day 7 in the lung, salivary gland, and pancreas, and by day 14 inflammatory lesions were found in almost all organs examined. Moderate to severe inflammation was not present until the mice were 10 to 14 days old. In the older animals, there was a slight increase in the severity of the inflammatory lesions as the mice aged. (Am J Pathol 1995, 146:276–288)

Transforming growth factor-β1 (TGF-β1) is a polypeptide homodimer with a molecular weight of 25 kd. TGF-β1 is a member of a closely related family of growth-and-differentiation regulatory peptides that includes TGF-β2 and TGF-β3. These in turn are members of a larger super family of TGF-β-like peptides that includes the activins and inhibins, the bone morphogenesis proteins, and the decapentaplegic and veg-related proteins.[1,2] TGF-β1 affects numerous physiological processes and elicits diverse cellular responses, having potentially both an inhibitory and stimulatory effect on the same cell, depending on the type of cell, its state of differentiation, and other environmental signals.[1,2] Thus, it has been suggested that TGF-β1 acts as a biological switch, a signaling molecule, coupling the cell to its environment and providing for plasticity of response.[3] One of the regulatory roles TGF-β1 plays is as a potent inhibitor of immune and inflammatory responses.[4] It inhibits cytotoxic T lymphocyte formation,[5] is an autocrine regu-

Supported by American Heart Association Grant SW-93-09-1 and NIH Grants PO1 HL4196, RO1 HD 26471, PO1 46826, and PO1 ES05652.

Accepted for publication September 16, 1994.

Address reprint requests to Dr. Gregory Boivin, Department of Pathology and Laboratory Medicine, Division of Comparative Pathology, University of Cincinnati College of Medicine, PO Box 670529, Cincinnati, OH 45267-0529.

latory agent in the suppression of T and B cell proliferation,[6] and is a regulator of the production of interferon-γ and tumor necrosis factor-α and -β3[6]. TGF-β1 also inhibits the regulation of multiple hematopoietic lineages in mice[7] and has shown promise in the treatment of autoimmune disorders such as experimentally induced encephalitis and collagen-induced arthritis.[8] A recurring functional role for TGF-β1 is one of growth inhibition; the standard assay for TGF-β1 is inhibition of growth of a mink lung epithelial cell line.[9] Most of the data accumulated on TGF-β1 have been established by *in vitro* studies. Recently, however, the generation and initial characterization of mice homozygous for a mutated TGF-β1 gene was described by our laboratories and others.[10,11] These mice provide a valuable *in vivo* model for examining TGF-β1 function.

TGF-β1-null mutant (knockout) mice became moribund at 15 to 36 days of age and exhibited a wasting phenotype that manifested itself by severe weight loss and a dishevelled appearance. These animals invariably died within a few days due to complications of cardiac, gastric, or diaphragmatic inflammatory lesions.[10,11] On the mixed 129/CF-1 background, gastric inflammation was often accompanied by hyperplastic epithelium and ulcers[10]; on the mixed 129/B6 background there was little gastric involvement.[11] Subsequent analysis of the latter mouse found elevated levels of major histocompatibility complex (MHC) antigen expression on day 6 and detectable levels of inflammation on day 9[12] suggesting that aberrant MHC expression may be primary to inflammation. Another study found increased leukocyte adherence to endothelium on day 7,[13] raising the question whether abnormal expression of adhesion molecules mediating leukocyte-endothelial cell interactions could be primary to inflammation. To help clarify these questions it is necessary to know when inflammation occurs in the various organs and tissues affected. The study presented here demonstrates that inflammatory lesions appear as early as day 5 in some organs and as late as day 14 in others. In the course of this study previously unreported hyperplastic epithelia were observed in several organs. The temporal relationship between the appearance of these mutant TGF-β1 phenotypes and inflammation was determined.

Materials and Methods

Animals

A breeding colony, derived from 129/CF-1 hybrids heterozygous for the mutant TGF-β1 allele, which contained TGF-β1-deficient homozygous, heterozygous, and wild-type mice, was housed in a barrier facility in high efficiency particulate air-filtered ventilated racks in microisolator cages (Lab Products, Maywood, NJ). Serological and histological examination of selected mutant and wild-type animals, as well as sentinel animals in the room, revealed no pathogenic organisms (bacterial, viral, mycoplasmal, or parasitic). Sera were tested at the University of Missouri Research Animal Diagnostic and Investigative Laboratory for mouse hepatitis virus, Sendai, pneumonia virus of mice, *Mycoplasma pulmonis*, Theiler's murine encephalomyelitis virus, Reovirus-3, minute virus of mice, polyoma virus, mouse adenovirus, ectromelia, lymphocytic choriomeningitis virus, epizootic diarrhea of infant mice virus, and cilia-associated respiratory bacillus. Microbiological examination was performed at the University of Cincinnati Medical Center Microbiology Laboratory. No bacterial pathogens were found in samples of cecum and trachea. Parasitic infestation in the mice was examined by anal tape testing, direct examination of cecal and colonic contents (pinworms), and direct examination of fur collected from around the ear (mites). There were no endoparasites or ectoparasites found with these tests.

Pathology

For the neonatal study, 10 mutant and 10 wild-type mice were euthanized and examined grossly and histopathologically on days 5, 7, 10, and 14 (day 1 is day of birth). Fifty-three moribund mutant mice, from 15 to 85 days of age, and 30 age-matched wild-type controls were also examined for the moribund mouse study. Organs collected for histopathological examination in the neonatal and moribund mice were heart, diaphragm, stomach, pancreas, mesentery, lung, spleen, thymus, salivary gland, and liver. In addition, in selected moribund animals, kidney, ureter, gall bladder, small and large intestine, adrenal gland, thyroid, lymph nodes, trachea, Harderian gland, ureter, urinary bladder, eye, skeletal muscle, cortex, cerebellum, and reproductive organs were examined. Tissue samples were fixed in 10% neutral buffered formalin, paraffin embedded, and sectioned at 5 μ thickness. Slides were stained with hematoxylin and eosin. The severities of the findings were scored on a 0 to 4 scale: 0, no findings; 1, mild; 2, moderate; 3, severe; and 4, very severe. Categories included inflammation for all organs; hyperkeratosis, hyperplasia, edema, and ulcer development in the stomach; myelopoiesis in the liver; and fibrosis and necrosis in the heart and diaphragm.

Morphometric analysis was performed to quantify lymphoid depletion of the spleen. A Macintosh Quadra 950 was used with system software 7.1, NIH Image 1.50 software, and a Scion Lg-3 frame grabber. Adobe Photoshop 2.5 was used occasionally to manipulate images, and Excel 4.0 was used to organize data and do calculations. The images were captured as TIFF files before analysis. NIH Image 1.50 was calibrated with a micrometer to convert pixels to millimeters for each objective of an Olympus BH-2 microscope. Analysis of entire cross sections of spleen involved manual selection of the white pulp regions and subsequent measurement of the selected area. Total area was measured by density slicing the gray scale values that correlated with the entire tissue region.

Mouse Weights

Twenty litters containing 21 mutants, 76 heterozygotes, and 28 homozygous wild-type mice were weighed daily during the working week, from birth to day 21. In addition, weights of the neonatal and moribund mice at the time of euthanasia were included. All weights were used to assess whether differences could be determined for weight gains of mutant mice *versus* wild-type mice, and to determine whether body weight could be correlated with initiation of lesions or lesion location. Values were analyzed by robust *t*-test with a one-tailed $\alpha = 0.05$.

Genotyping

All mice used in this study were genotyped by polymerase chain reaction analysis of tail DNA samples collected from pups at 2 to 7 days of age. A small portion of the tail was incubated overnight at 56 C in lysis buffer (100 mmol/L Tris-HCl, pH 8.5; 5 mmol/L EDTA, pH 8.0; 200 mmol/L NaCl; 0.2% sodium dodecyl sulfate; and 18 μl proteinase K at 20 mg/ml). The following day the sample was centrifuged and the supernatant extracted once with phenol/chloroform and once with chloroform. The DNA was precipitated with an equal volume of isopropanol and then resuspended in 400 μl of TE (10 mmol/L Tris-HCl, 1 mmol/L EDTA, pH 8.0). The concentration of the DNA was between 200 and 400 ng/μl. A total of 1 μl of the sample was added to 18 μl of primer mix containing 9.5 μl H_2O, 2.0 μl 10X polymerase chain reaction buffer (Boehringer Mannheim, Indianapolis, IN, or Perkin-Elmer, Norwalk, CT), 2.0 μl MgCl (final concentration at 2 mmol/L), 1.0 μl of each dNTP (final concentration of each at 0.5 mmol/L), and 0.25 μl of each primer (0.25 μmmol/L final concentration; upstream, 5′-GAGAAGAACTGCTGTGTGCG-3′; downstream, 5′-GTGTCCAGGCTCCAAATATAGG-3′). These primers will amplify a 142-bp fragment of exon 6 from a wild-type TGF-β1 allele and a 1247-bp fragment from a mutant TGF-β1 allele harboring the neomycin insert. The solution was overlaid with 50 μl of mineral oil and heated to 95 C for 3 minutes. The solution was cooled to 58 C and 1 μl of Taq polymerase (Boehringer Mannheim or Perkin-Elmer) was added. The solution was remelted at 95 C for 1 minute, annealed at 58 C for 2 minutes, and extended at 72 C for 3 minutes in an Ericomp apparatus. The cycle was repeated 30 times. Running dye was added to the final samples. The samples were analyzed on a 4% NuSieve gel run at 80 V for 1 hour and stained with ethidium bromide.

Electron Microscopy

Sections of heart were collected from 5-day mutant and wild-type mice (2 and 4, respectively) and 7-day mutant and wild-type mice (4 and 2, respectively). The cardiac tissue was fixed in 2% glutaraldehyde for 4 hours, then transferred into cacodylate buffer. Tissues were post-fixed with osmium tetroxide. Thick sections (1 μ) were prepared and stained with toluidine blue. Thin sections (70 to 80 Å) were stained with lead acetate. Examination of sections and photographs were taken with a Hitashi H600 microscope.

Flow Cytometry

Mouse thymocytes were harvested from intact thymus via mild disruption on glass microscope slides and 1 × *g* sedimentation in 10 ml of staining media buffer (SMB; phosphate-buffered saline plus 0.1% sodium azide and 4% fetal bovine serum) on ice. Supernatant containing thymocytes was transferred to a fresh 10-ml tube and spun at 1000 rpm at 0 to 4 C for 10 minutes. The supernatant was removed and the cells were resuspended in 1 to 5 ml of SMB. Cells were counted and 1.6×10^6 cells per staining reaction were aliquotted. Cells were pelleted, the supernatant removed, and 1 μg of each antibody was added in 20 μl of SMB at 0 to 4 C (antibodies to CD4, CD8a, and TCRab were purchased from PharMingen, San Diego, CA, and used without modification). Staining for 45 minutes at 0 to 4 C in the dark was followed by washing (200 μl of SMB) and spinning (1000 rpm) for three cycles. Cells were suspended in 200 μl of SMB containing 5 μg/ml propidium iodide to screen out

nonviable cells (there was 90% viability of cells). The suspension was diluted further with 800 μl of Isoton II (Becton Dickinson, San Jose, CA) at 0 to 4 C, filtered through 50-μ nylon mesh, and analyzed on a Becton Dickinson FACScan with Lysis II software.

Results

During the course of this study, 806 mice were born to 129/CF-1 parents heterozygous for the mutant TGF-β1 alleles. Of these, 113 were homozygous mutants, 413 were heterozygous, and 280 were homozygous wild-type mice. Thus, instead of the expected 25%, only 14% of the mice born to heterozygous parents were homozygous deficient for TGF-β1.

Mutant mice were born virtually indistinguishable from their homozygous wild-type and heterozygous littermates. Clinically and grossly there were no differences observed in the neonatal mice except for body weight values. Weights of the mutant mice were significantly lower than those of the wild-type mice at birth ($P < 0.05$) and at several time points during the first weeks of life (Figure 1). On the average, mutant mouse weight gains paralleled the wild-type gains and peaked around day 15, then declined through weaning. Organ weight to body weight ratios were examined for the heart, spleen, and thymus (Table 1). Heart to body weight ratios were significantly increased in the 7-, 10-, and 14-day mutant mice. Spleen to body weight ratios were also significantly increased compared with wild-type controls beginning on day 7. The thymus weights and thymus to body weight ratios of mutant and wild-type mice were not significantly different.

Most mutant mice died or were euthanized when moribund between 15 and 36 days of age. Of the 93 mutant mice examined, 2 lived past 40 days of age and 1 mouse lived 85 days. Examination of these mice revealed that the TGF-β1-deficient moribund mice exhibited a moderate to severe, multifocal, organ-dependent mixed inflammatory cell infiltration, adversely affecting the heart, stomach, diaphragm, liver, lung, salivary gland, and pancreas. The development and characterization of the histopathological changes of the 40 mutant neonatal mice and the 53 older moribund mice are presented by age in the following paragraphs and are summarized in Table 2. No significant lesions were observed in the wild-type control mice, nor were there any lesions in the kidney, ureter, gall bladder, urinary bladder, thyroid, eye, Harderian gland, adrenal gland, brain, intestine, or reproductive tract of the moribund mutant mice.

Histopathology

Inflammatory lesions were first observed in the heart of a 5-day mutant mouse. The lesion was characterized by a mild, focal, lymphocytic infiltrate in the atria (Figure 2). In general, the myocardial cells in the 5-day mutant mice had a much more basophilic cytoplasm than those of the wild-type animals, which may indicate increased ribosomal activity in the cytoplasm. No other inflammatory lesions were evident

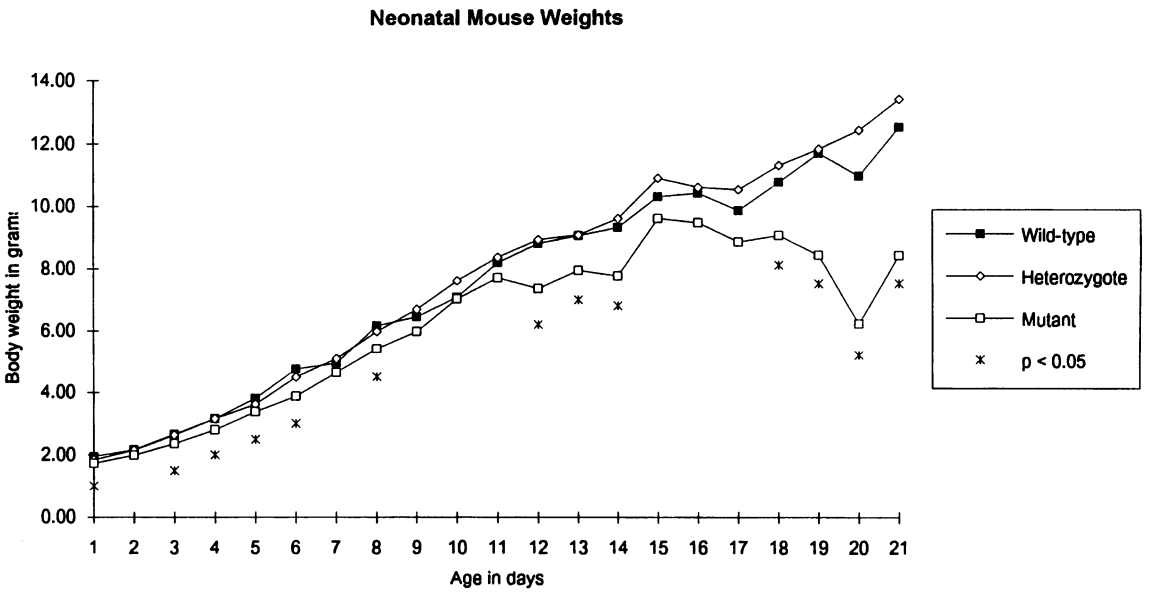

Figure 1. *Body weight in grams of wild-type, heterozygous, and TGF-β1-null mutant neonatal mice.*

Table 1. *Body Weight and Organ Analyses of TGF-β1-Deficient and Wild-Type Neonatal Mice*

	Day 5		Day 7		Day 10		Day 14	
	Mutant	Wild-Type	Mutant	Wild-Type	Mutant	Wild-Type	Mutant	Wild-Type
Body Wt. (g)*	2.7 ± 0.2†	4.1 ± 0.1	4.3 ± 0.2	4.7 ± 0.2	6.7 ± 0.3	6.9 ± 0.2	7.4 ± 0.4	8.3 ± 0.5
SW/BW (%)[2]	0.55 ± 0.07	0.58 ± 0.03	0.90 ± 0.05†	0.55 ± 0.04	1.09 ± 0.05†	0.62 ± 0.03	1.16 ± 0.11†	0.54 ± 0.04
WP (%)[3]	9.0 ± 1.94‡	15.1 ± 2.0	9.8 ± 1.3†	18.6 ± 2.6	11.5 ± 1.3†	21.8 ± 2.4	22.9 ± 3.1	28.0 ± 3.7
HT/BW (%)[4]	0.75 ± 0.04	0.73 ± 0.05	0.76 ± 0.02‡	0.69 ± 0.03	0.91 ± 0.05‡	0.74 ± 0.06	0.97 ± 0.04†	0.74 ± 0.03
TW/BW (%)[5]	0.47 ± 0.03	0.51 ± 0.03	0.57 ± 0.04	0.54 ± 0.03	0.59 ± 0.03	0.66 ± 0.04	0.68 ± 0.05	0.67 ± 0.05

Body wt. (g), body weight in grams ± SE; SW/BW, spleen weight to body weight ratio (% ± SE); WP, white pulp area in spleen (% ± SE); HT/BW, heart weight to body weight ratio (% ± SE); TW/BW, thymus weight to body weight ratio (% ± SE).

* All groups have 10 animals except day 5 mutant white pulp, day 5 mutant TW/BW, day 10 mutant TW/BW, and day 10 wild-type TW/BW, which contain 9, 9, 8, and 9 each, respectively. Statistical significances of animal body weights may be different than seen in Figure 1 as different subsets of mice were analyzed.

† Significantly different from wild-type control at $P < 0.01$.

‡ Significantly different from wild-type control at $P < 0.05$.

Table 2. *Incidence and Severity of Lesions in TGF-β1-deficient and Wild-Type Mice*

	Day 5		Day 7		Day 10		Day 14		Days 15–20		Days 21–29		Days 30–85*	
	Mutant	Wild-Type	Mutant	Wild-Type	Mutant	Wild-Type	Mutant	Wild-Type	Mutant	Wild-Type	Mutant	Wild-Type	Mutant	Wild-Type
Heart	1/10†	0/10	4/10	0/10	9/10	0/9	10/10	0/10	18/18	0/7	18/22	0/12	9/10	0/10
	1.0‡	0.0	0.5	0.0	1.1	0.0	1.5	0.0	1.6	0.0	1.8	0.0	1.9	0.0
Diaphragm	0/10	0/10	0/10	0/10	4/10	0/10	6/10	0/10	7/15	0/7	10/15	0/8	7/10	0/9
	0.0	0.0	0.0	0.0	0.8	0.0	1.2	0.0	1.3	0.0	2.2	0.0	2.3	0.0
Stomach	0/10	0/10	0/10	0/10	1/10	0/10	4/10	1/10	13/16	0/8	20/23	0/12	9/11	0/10
	0.0	0.0	0.0	0.0	0.5	0.0	0.9	0.5	2.4	0.0	2.4	0.0	2.9	0.0
Pancreas	0/10	0/8	5/10	0/10	7/10	0/10	9/10	0/10	9/13	0/8	11/19	0/11	4/8	0/10
	0.0	0.0	0.5	0.0	1.4	0.0	1.5	0.0	1.5	0.0	1.8	0.0	1.8	0.0
Mesentery	3/10	2/10	0/10	0/10	7/10	0/10	8/10	0/10	8/12	2/8	19/22	3/12	9/11	4/10
	0.8	0.5	0.0	0.0	1.1	0.0	1.3	0.0	1.0	0.5	1.2	0.7	1.1	0.6
Lung	1/10	0/10	2/10	0/10	8/9	0/10	6/10	0/10	15/16	0/8	14/24	0/12	7/10	0/10
	0.5	0.0	0.8	0.0	1.8	0.0	1.8	0.0	1.4	0.0	2.0	0.0	1.2	0.0
Salivary	0/10	0/10	1/8	0/10	3/10	0/10	3/10	0/10	2/7	0/8	11/14	0/12	3/7	0/10
Gland	0.0	0.0	0.5	0.0	0.8	0.0	0.8	0.0	1.3	0.0	1.4	0.0	1.7	0.0
Liver	8/10§	8/10	9/10	8/10	9/10	6/10	9/10	1/10	15/16	1/8	23/23	0/12	9/11	0/10
	1.3	1.0	0.9	0.9	1.3	0.9	1.3	0.5	1.6	1.0	2.0	0.0	1.8	0.0

* Only three mice lived past day 36 (to days 40, 42, and 85). Day 1 is day of birth.

† Number with lesions/number examined.

‡ Mean score of animals with lesions. Lesion Scoring: 0, no lesions; 1, mild; 2, moderate; 3, severe; and 4, very severe.

§ Incidence and severity of periportal myelopoiesis and lymphocytic infiltration.

in 5-day mice; however, increased myelopoiesis was first evident at this age. The most significant change was an almost two-fold increase in the number of myelopoietic cells in the liver parenchyma of mutant mice. There was also a moderate decrease in the amount of thymic cortex present in the mutant animals starting at 5 days of age.

Inflammatory lesions became more prevalent in the mutant mice at 7 days of age, involving the lung, salivary gland, liver, and pancreas (Figure 3 and 4). There was a mild lymphocytic infiltrate observed between muscle fibers of the atrial and ventricular myocardium in 4 of 10 mice. Perivascular lesions were seen in the lungs of 2 of 10 mice, and periductal, perivascular and diffuse lesions in the salivary gland in 1 of 8 mutant mice. A mild multifocal to diffuse interstitial infiltrate of neutrophils was observed in the pancreas of 5 of 10 mutant mice. Increased myelopoiesis continued to be present in the liver, accompanied by a mild periportal lymphocytic infiltrate. There was also a continued decrease in the thymic cortex cellularity.

At 10 days of age, lesions increased in incidence and severity in nearly all organs examined. Inflammatory lesions were seen in the heart (9 of 10), diaphragm (4 of 10), pancreas (7 of 10), salivary gland (3 of 10), and lung (8 of 9). Lesions consisted of very mild to moderate, focal to multifocal, primarily lymphocytic infiltration with occasional neutrophils. Additional lesions were seen in the pancreas and lungs of 2 and 4 mutant mice, respectively. The pancreatic lesions were characterized by a severe lymphocytic infiltration with focal necrosis of the exocrine pancreas. In the lungs of 4 10-day (and 1 14-day) mutant mice, there were large pleomorphic lymphoid aggregates with plasma cells, pneumocyte hyperplasia, histiocytosis, and areas of focal abscesses with giant cell infiltration primarily in the peribronchiolar and perivascular regions. In the wild-type littermates the

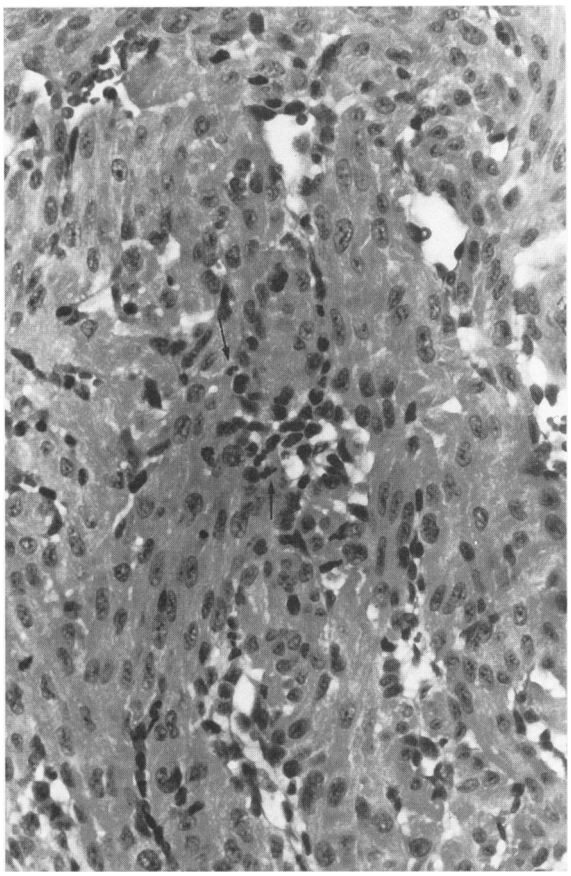

Figure 2. *Heart from 5-day TGF-β1-deficient mutant mice showing focal neutrophilic infiltration (arrows). H&E; original magnification, ×400.*

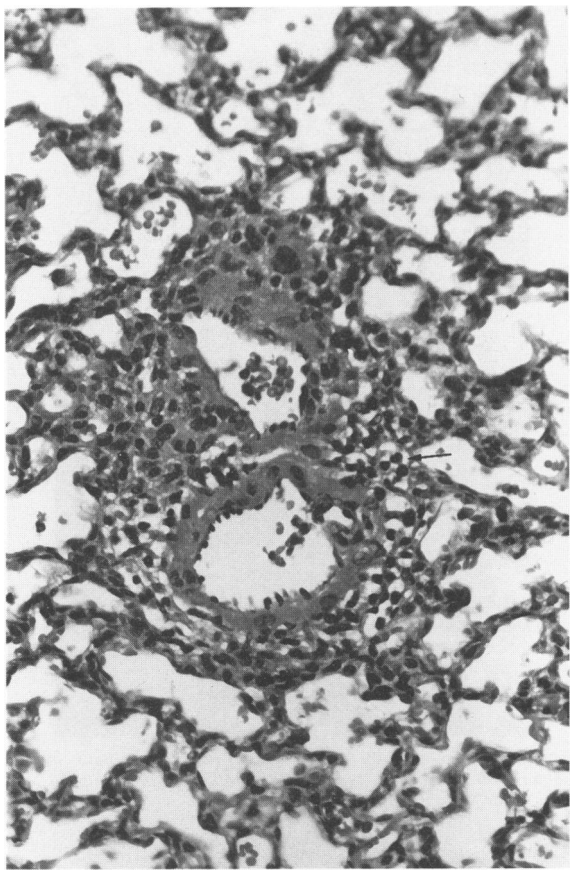

Figure 3. *Lung from 7-day TGF-β1-deficient mutant mouse. There was mild perivascular lymphoid cuffing (arrow). H&E; original magnification, ×200.*

amount of periportal granulopoiesis began to decline on day 10. In the mutants the periportal granulopoiesis remained the same or increased and was markedly increased over that seen in the controls. In addition, 7 of 10 mutants had multifocal mature and immature lymphocytic infiltration into the mesentery around the pancreas and other abdominal organs. It was not clear whether this was an inflammatory or myelopoietic infiltration.

Fourteen-day mutant mice were the first to show gastric lesions. The mutant mice had a mild, diffuse, lymphocytic infiltrate into the submucosa of the nonglandular region (4 of 10) and into the submucosa of the glandular region (1 of 10). Lymphocytic inflammatory changes in the other organs progressed in severity and incidence, including the heart (10 of 10), diaphragm (6 of 10), pancreas (9 of 10), and salivary gland (3 of 10). In addition to these lesions, there were several other changes in organs that were first seen on day 14. Associated with the pancreatic inflammation, was a mild to moderate edema that separated lobules. There was a moderate, diffuse, lymphocytic, interstitial pneumonia associated with the peribronchiolitis in the mutant mice. Two mutant mice had biliary duct hyperplasia in the liver in addition to the lymphocytic infiltrate and granulopoiesis. Eight of ten mutants had a moderate lymphocytic infiltrate into the mesentery. Increased myelopoiesis continued in the mutant mice as did the thymic cortical depletion.

Lesion severity in moribund mice was increased over that seen in the neonatal mice yet remained highly variable. The lesion severity also increased in the moribund animals as they aged. The lymphocytic inflammation continued to be the most severe change in the heart (45 of 50), diaphragm (24 of 40), pancreas (24 of 40), stomach (42 of 50), mesentery (36 of 45), lungs (36 of 50), and skeletal muscle (16 of 28). In contrast to the neonatal mice, lymphocytic infiltration in the moribund mice was frequently accompanied by additional inflammatory cell types. In the heart, the additional inflammatory cells included macrophages, neutrophils, plasma cells, and fibrocytes; in the stomach and pancreas there were abundant neutrophils; and in the lungs there were giant cells, histiocytes, and neutrophils.

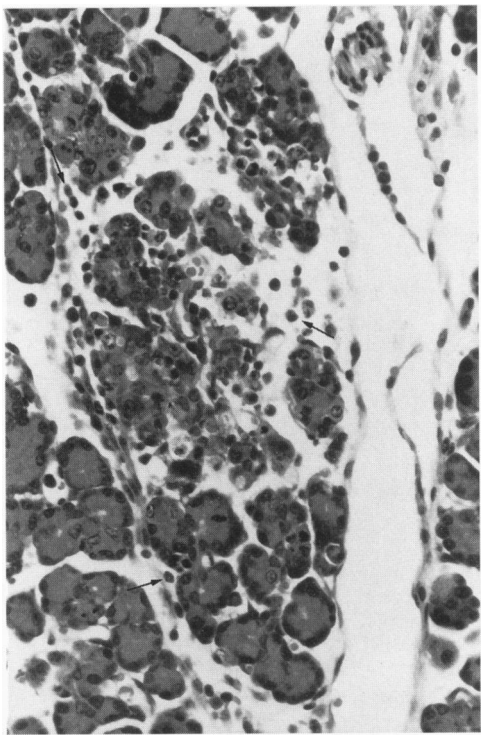

Figure 4. *Pancreas from 7-day TGF-β1-deficient mutant mouse demonstrating the earliest neutrophilic inflammatory infiltrate (arrows). H&E; original magnification, ×200.*

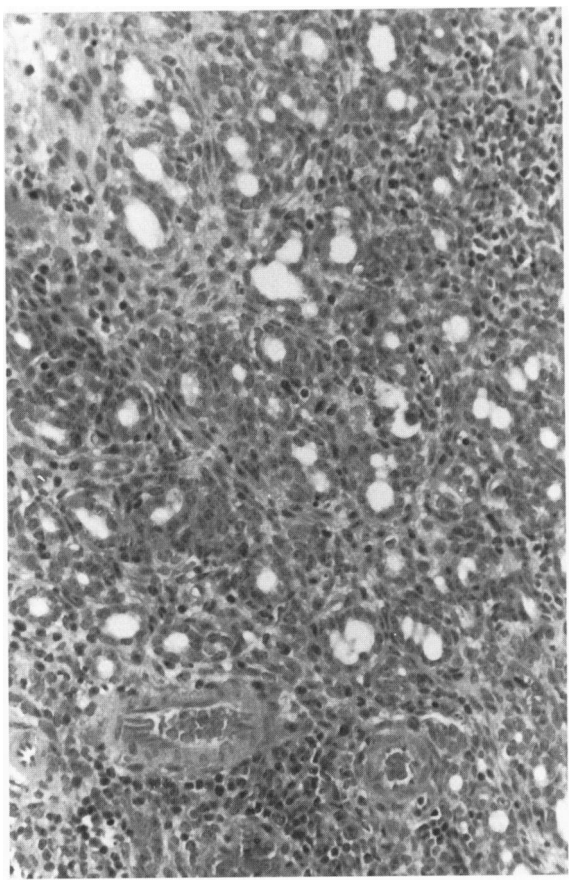

Figure 5. *Pancreas from 19-day mutant mouse with generalized hyperplasia of the ductal epithelium and diffuse lymphocytic infiltration. H&E; original magnification, ×200.*

In addition to the inflammatory cell infiltrate, there were additional changes worthy of note. There was moderate focal ductal hyperplasia of the pancreas (5 mice; Figure 5) and the salivary gland (1 mouse) and bile duct proliferation and severe fibrosis of the periportal areas in the liver (4 mice; Figure 6). In addition to the chronic diffuse perivasculitis seen in the neonatal lung, peribronchiolitis (8 of 50) and vasculitis (3 of 50) were observed in the moribund mice. Periportal granulopoiesis and lymphocytic proliferation in the liver was seen in 47 of 50 moribund mutant mice. Five mice had severe multifocal peracute coagulative necrosis of the liver.

There was also a continued increase in the multifocal extramedullary myelopoiesis in the liver of the mutant mice. The lymph nodes of moribund postweaning mice were enlarged in 23 of 36 mice and hyperplastic in 10 of 36 mice. The change in lymph node cellularity was not observed in neonatal mutant mice.

There was myocardial cell necrosis in 5 of 50 mice and marked fibrosis of the heart in 1 mouse. Dilation of the right ventricle and congestion in the liver compatible with congestive heart failure were seen in 1 mouse. Other changes consistent with congestive heart failure were also seen in the lung (congestion in 4 mice and edema in 2 mice) and liver (congestion in 2 mice). Five moribund mutant mice had atrial thrombi. Moderate fibrosis was seen in the most severely inflamed mutant mouse diaphragms.

Severe stomach lesions were found in 46% of moribund TGF-β1-deficient mice (scores ≥2.5). The lesions were characterized by mild to severe, focal to multifocal ulceration (24 of 50), mixed lymphocytic and neutrophilic gastritis (42 of 50), hyperkeratosis (36 of 50), edema (27 of 50), and epithelial cell hyperplasia (30 of 50) of the nonglandular region and the glandular-nonglandular junction of the stomach. Ulcers involved the glandular-nonglandular junction of the stomach in 17 of the 24 affected mice. No ulcers were seen solely in the glandular region. In the more severely affected stomachs, there was also a mild lymphocytic infiltration into the glandular submucosa. In 10 mutant mice there was severe dysplasia of the nonglandular stomach epithelium, forming isolated nests of dysplastic cells within the submucosa. Four of these lesions could be interpreted as squamous cell carcinomas. However, none of the lesions

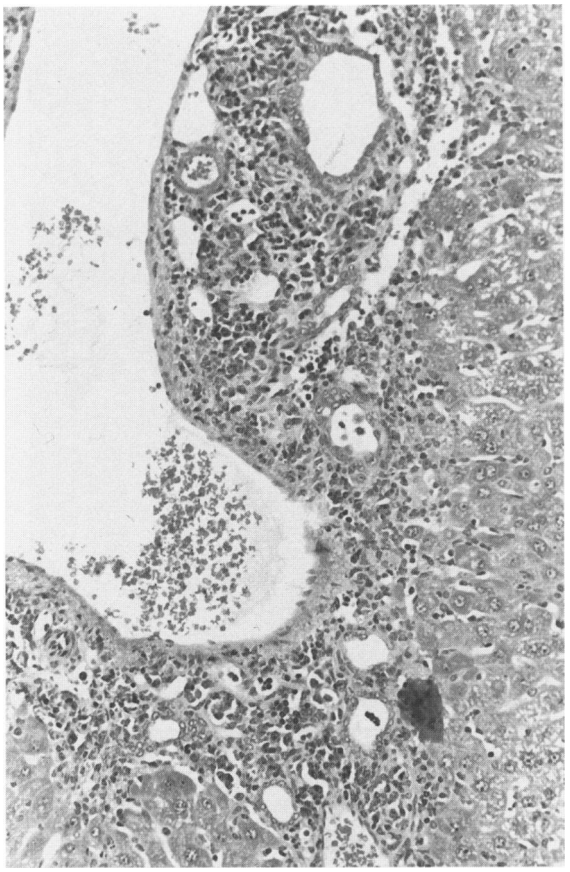

Figure 6. *Liver from 33-day TGF-β1-deficient mouse with biliary hyperplasia, granulopoiesis, and lymphocytic infiltration. H&E; original magnification, ×200.*

showed evidence of metastasis nor were there any abnormal mitotic figures observed.

Electron Microscopy

Ultrastructural differences were detected by electron microscopy in 5- and 7-day mutant mice. In 5-day mutant mice, most myocytes appeared normal. However, a few myocytes had evidence of mitochondrial changes characterized by decreased numbers of cristae. In 7-day mutant mice, changes were more numerous including evidence of randomly displaced myofilament bundles and a pronounced swelling of mitochondria harboring few cristae (Figure 7). None of these changes were seen in the 5- and 7-day wild-type mice. In addition, several nuclei in the 7-day mutant hearts contained DNA clumping, which was seen infrequently in the wild-type mice.

Morphometric Analysis

Changes in the spleen included a decreased population of lymphoid tissue in the white pulp in all ages of neonatal mutant mice. The spleens were characterized by a decreased density of lymphocytes in the lymphoid nodules and a decrease in the area of white pulp. Morphometric analysis of the spleens revealed approximately a 50% decrease in white pulp area in the 5-, 7-, and 10-day mutant mice and a 25% decrease in the 14-day mice (Table 1). In contrast, spleens of mutant mice were consistently 1.5 to 2 times heavier than those of wild-type littermates in all age groups examined. This was attributed to a marked increase in extramedullary myelopoiesis in the red pulp.

Flow Cytometry

Comparisons of mutant and wild-type littermate thymuses were performed on 9-day and 21-day mice via flow cytometry (fluorescent-associated cell analysis). The 9-day mice showed minimal differences in their CD4 and CD8a populations relative to one another, although a slight skewing of the mutant 9-day thymocytes in favor of the $CD4^+CD8a^-$ phenotype could be detected (Figure 8A, B). Unlike wild-type mice, moribund 21-day mice were depleted of $CD4^+CD8a^+$ (double-positive) immature thymocytes (approximately 70% in the wild-type and 3% in the mutant mice) and had increased $CD4^+CD8a^-$ mature cells (approximately 7% in the wild-type and 55% in the mutant mice; Figure 8C, D). The predominant thymocyte phenotype in moribund (21-day) mutant mice was $TCR\alpha\beta^+$(bright)$CD4^+CD8a^-$. This change in T cell populations is consistent with a stress profile similar to that observed in graft rejection and also in moribund or sick animals.[14]

Discussion

In an attempt to understand the roles played by TGF-β1 in the whole mammalian organism, we generated TGF-β1-deficient mutant mice.[10] Because of the multiple lesions presented in these mice, the most prevalent of which was inflammation, the question arises as to the degree to which the noninflammatory disorders are primary or secondary to the inflammation. Ascertaining the onset and progression of the various types of lesions found in the mutant mice establishes baseline data to begin to address this question.

Inflammatory cell infiltration was first observed in 5-day mutant mice in the heart, and by day 10 inflammation was seen in almost all organs examined (gastric lesions were not seen until day 14). Moderate to severe lesions were not present until the mice were

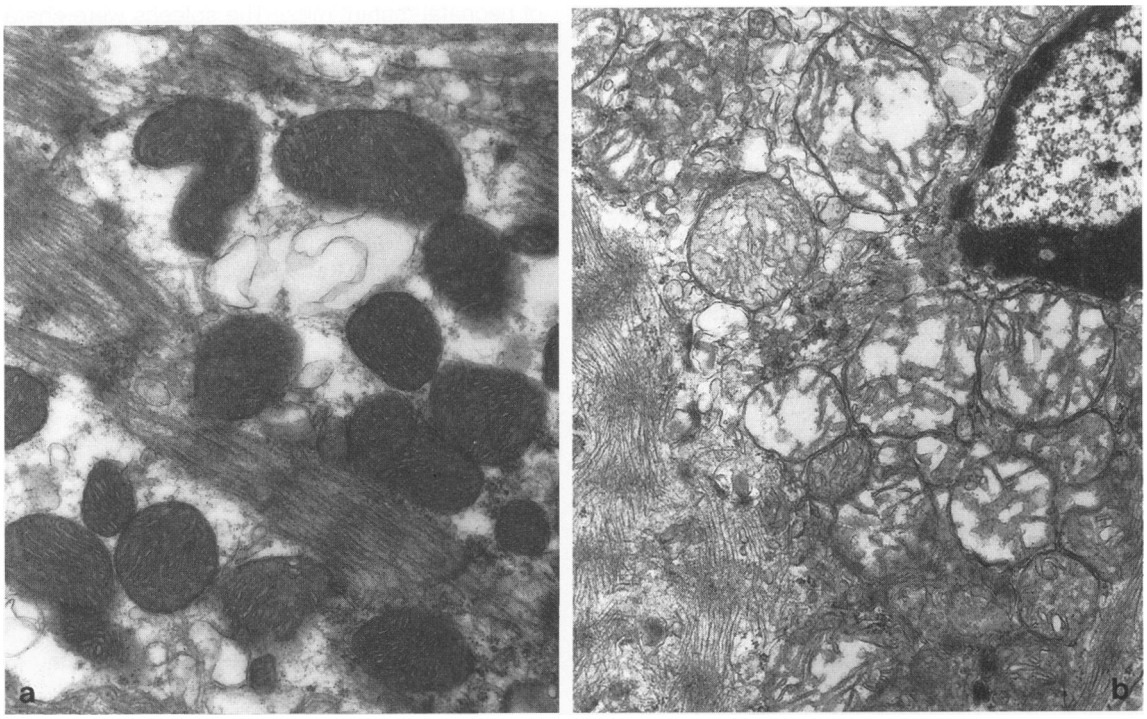

Figure 7. *Transmission electron microscopic photo of wild-type and mutant hearts.* A: *Normal myocardium from a 7-day wild-type mouse.* B: *Increased nuclear chromatin clumping (top right), fragmentation of filaments (bottom left), and mitochondrial swelling in myocytes from a 7-day mutant heart. These changes were more common in the mutant mice and are consistent with increased cell division in the mutant mice. Lead acetate; original magnification, ×17,000.*

10 to 14 days old. Ultimately, in the older mice, the severity of the lesions increased to the point at which weight loss began and death ensued. Death occurred in all but three mice before 35 days of age. All mice died by 85 days of age.

In the mutant hearts, ultrastructural alterations in some cardiac myocytes were first observed on days 5 and 7. These lesions coincided with the appearance of the first early inflammatory changes detected by light microscopy. The ultrastructural alterations included myofibrillar displacement and apparent enlargement of mitochondria with a reduction in the number of cristae. These characteristics are similar to what is observed ultrastructurally in cardiac myocytes undergoing mitosis.[15] During the neonatal period, TGF-β1 increases in the myocardial compartment of the wild-type mouse, coinciding with the cessation of cardiac myocyte mitosis. This period also coincides with the hyperplastic to hypertrophic growth switch that normally occurs at this time.[16] Therefore, the lack of TGF-β1 may allow prolongation of the hyperplastic phase of cardiac growth. Additional support for this interpretation is the observation that there is abnormal cardiac development in four homozygous mutant pups from a TGF-β1 homozygous mutant mother rescued with daily injections of dexamethasone. In the mutant dam there is elimination of maternally supplied TGF-β1 to the developing mouse. The cardiac lesions in the four neonates were characterized by a disordered proliferation of myocytes with poor ventricular lumen development and atrioventricular junction abnormalities.[17] However, a causative role for inflammation or dexamethasone in the context of TGF-β1 deficiency cannot be ruled out.

The occurrence of lymphocytic infiltration in the mutant hearts, with myocyte degeneration and accompanying elevated inflammatory cytokines may also bring about some of the ultrastructural changes observed.[18] Elevated levels of proinflammatory cytokines such as interferon-γ, tumor necrosis factor-α, interleukin-1β, and macrophage inflammatory protein-1α were found in moribund mutant mouse tissues.[10] In contrast, interferon-γ levels in neonatal hearts were similar between mutant and wild-type animals as measured by mRNA expression.[12] MHC I and II levels were elevated in a number of tissues, including the heart, before or at the time of inflammatory infiltration on day 9, implicating aberrant MHC expression as a possible mechanism giving rise to the immunopathology observed in the TGF-β1 mutants.[12] Our data shows that inflammation can already be present at that age; consequently it is possible that aberrant MHC expression is secondary to inflammation.

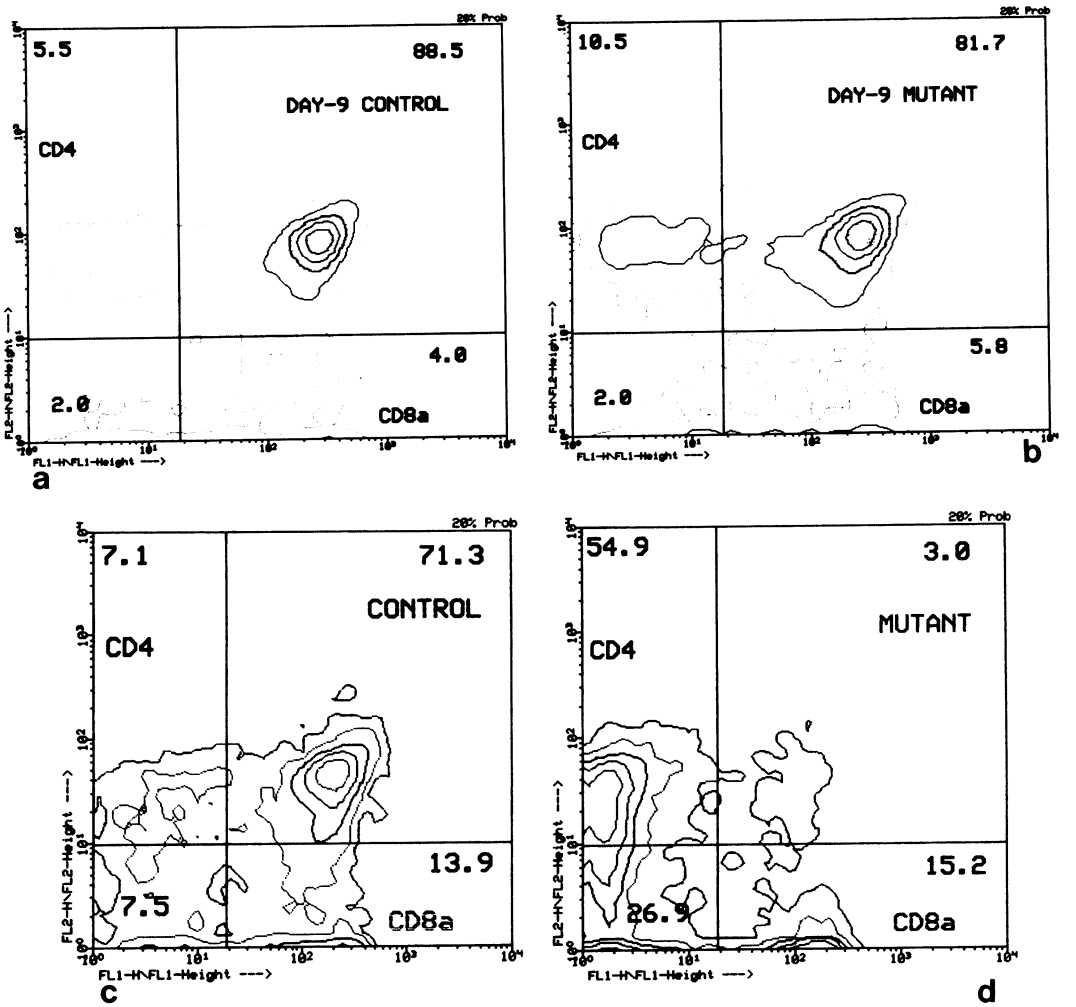

Figure 8. *Topographic plot of CD4 and CD8a populations for mutant and wild-type mice (10,000 cells; y axis depicts CD4 expression and x axis depicts CD8a expression, with percent of total shown for each quadrant).* A: *Thymus from a 9-day wild-type mouse. There is a normal distribution of lymphocytes with numerous CD4$^+$ CD8a$^+$ cells.* B: *Thymus from a 9-day mutant mouse. Predominance of CD4$^+$ CD8a$^+$ cells, with a mild increase in the CD4$^+$ CD8a$^-$ mature cells.* C: *Thymus from a 21-day wild-type mouse. There is a normal distribution of lymphocytes with numerous CD4$^+$ CD8a$^+$ cells.* D: *Topographic plot of CD4 and CD8a populations for the 21-day mutant mouse. There is a shift to single positive CD4$^+$ CD8a$^-$ mature cells and a loss of CD4$^+$ CD8a$^+$ immature cells.*

Mild gastric lesions were first observed at 14 days of age. Severe ulceration was seen as early as day 16. TGF-β1 aids in the healing of gastrointestinal mucosal injuries by stimulating migration of epithelial cells from the edges of the lesion.[19,20] The inability of the mutant mice to respond to ulcer development may be due to the failure of restitution of the mucosal epithelium. However, *in vivo* modeling of the role of TGF-β1 in mucosal healing is not well characterized and additional studies of this mutant mouse may contribute to a better understanding of ulceration and healing.[20]

In all animals, ulcers are thought to occur because of increased acid secretion, increased gastrin secretion, and/or a breakdown in the gastric- or duodenal-mucosal mucus barrier.[21] As none of the wild-type control mice developed ulcers, there is a relationship between ulcer development and the absence of TGF-β1. However, the mechanism will need to be established in additional studies. Several factors may be affecting the delicate balance of the gastric mucosa and its acidic contents in the mutant mouse, including mucosal immunity, bacterial infiltration, mucosal hyperplasia, altered acid secretion, altered mucus secretion, stress, and hyperkeratosis. Because cultures of the stomachs of several mutant and wild-type mice were negative for aerobic bacteria and *Helicobacter* species, bacteria are unlikely to play a role in the ulcer development.

Interestingly, C57BL/6J mice with a different targeted mutation also leading to TGF-β1 deficiency did not develop gastric ulcers but did have colonic and gastric necrosis.[11] These particular changes were

not seen in our animals. The difference in the lesion development between the two colonies may be due to a difference in microbial flora of the mice, a difference in the TGF-β1 mutation, or an intrinsic difference in genetic background of the two lines of mice.

To examine this potential genotypic difference with respect to lesion development, we crossed our TGF-β1-targeted mutation onto a 129/B6 mixed background and examined nine moribund mice carrying the TGF-β1 null mutation. These mice had all the pathological lesions seen in the 129/CF-1 strain yet only one had an ulcer (data not presented). This finding and other preliminary data from our laboratory suggest that the genotype of the mouse plays a major role in determining the effect of TGF-β1 deficiency on the host animal. Thus, the elimination of TGF-β1 is not the sole determinant for pathological changes, but rather the lesions are also influenced by other genetically encoded factors.

A recent investigation reported that mRNA coding for histamine, muscarine, gastrin, and dopamine receptors in the stomach are located in the inflammatory cells (macrophages, lymphocytes, and plasma cells) of the lamina propria and not in the parietal cells as had been generally assumed.[22] This observation would indicate that regulation of ulcer development is associated with inflammatory cells. In the TGF-β1-deficient mice, the submucosal leukocytic infiltration is greatly increased over that of wild-type animals and is present before ulcers are seen. If these cells have increased or altered receptor affinity, this change could produce an imbalance in the normal gastric secretions (ie, increased acid production or decreased mucus production) and thus initiate ulcer development.

In addition to the prominent nonglandular epithelial hyperplasia, dysplasia, and squamous cell carcinoma in the stomach, there was also epithelial hyperplasia in the salivary gland, pancreas, and liver of mutant mice. This hyperplasia correlates well with the well defined role of TGF-β1 as an inhibitor of epithelial cell growth *in vitro*.[23] Also, in 129/B6 mutant mice there was increased BrdUrd labeling in the basal cells of the epidermis.[23] Except for the latter, *in vivo* epithelial hyperplasia was always found in association with inflammation. The classification of the dysplastic epithelium of the stomach nonglandular mucosa to neoplastic epithelium is equivocal. Without evidence of metastasis, muscular mucosal invasion, or abnormal mitotic figures the identification of the lesion as a carcinoma is still potentially early. Continued analysis of the dysplastic gastric epithelium is going on to confirm the neoplastic nature of these areas.

Periportal granulopoiesis in the liver was present very early in both normal and mutant neonatal mice. The increased numbers of granulopoietic cells in the periportal area in the mutant mice of 7 days and older, as well as the increase in parenchymal myelopoietic cells, was attributed to the absence of TGF-β1 inasmuch as TGF-β1 has an inhibitory effect on myelopoiesis *in vitro*.[24,25] In addition, in the mutant mice, the periportal cell population progressed to a lymphocytic infiltration with bile duct hyperplasia. Because the lymphocytic infiltrate could be a response to an infectious agent, several mutant and normal livers were cultured. No pathological bacteria were detected. Steiner's stain for *Helicobacter hepaticus* in the livers of several mice was also negative. Titers to all known viral pathogens of mice were also negative.

Because an infectious agent was unlikely, other causes were considered. In the older mice, the presence of a variety of mature and immature leukocytes suggests that lesion development is partly due to myelopoiesis. The inflammation could also be due to an inability to regulate the immune response in the absence of TGF-β1.

From day 5 through moribundity, there was a decreased cellularity in the thymic medulla and white pulp of the spleen. This depletion may be due to increased recruitment of cells to other tissues or a decreased production of lymphocytes by these organs. The former is more likely as there is active recruitment to other locations in the mouse. There was also an increase in the weight of the spleens of the mutant mice. This was attributed to hematopoiesis and myelopoiesis suggesting excessive production of red and white blood cells. This is consistent with the role of TGF-β1 in early development as an inhibitor of myelopoiesis.[24,25] Increased circulating levels of neutrophils and monocytes have been previously reported in moribund mutant mice[10] and is consistent with the increased myelopoiesis. The hyperplasia and increased size of the lymph nodes is also consistent with this lack of inhibition due to the absence of TGF-β1.

Salivary gland adenitis was seen in several mutant mice by day 7. The lesions were characterized by a lymphocytic infiltrate followed by necrosis and neutrophil influx. The greatest amount of infiltrate was consistently around the ducts. This pleomorphic, periductal, lymphocytic, salivary adenitis has similarities to that seen in Sjogren's syndrome (N. Talal, personal communication).[26] Interestingly, in addition to the salivary gland lesions, several other less common lesions of Sjogren's disease were similar to lesions in the mutant TGF-β1 mice, including acute and chronic pancreatitis, chronic active hepatitis, and mild peri-

portal fibrosis.[27] In addition, Sjogren's patients may have stomach dyspepsia, chronic atrophic gastritis, alveolitis, respiratory vasculitis, and pseudolymphoma.[27] This syndrome emphasizes the diversity of lesions that are possible with a single autoimmune disease and may prove to be of importance in understanding the pathogenesis of disease in the mutant TGF-β1 mice and, concurrently, in understanding autoimmune diseases such as Sjogren's syndrome.

Although neonatal mutant mice were outwardly phenotypically normal, as previously reported,[10,11] there was a small but significant difference in their weights starting at birth. There were no significant clinical correlations with the location of lesions and weight loss. This lack of correlation may have been due to the number of animals in the study but more likely is due to the diversity of the presentation of the lesions in the mice.

Summary

This study establishes the time of onset of the inflammatory response in various tissues. With this information base it will now be possible to investigate the roles played by TGF-β1 in the regulation of many growth and differentiation processes by studying preinflammatory tissues.

The earliest observed inflammatory cell responses were found on day 5 in the heart, day 7 in the lung, pancreas, and salivary gland, day 10 in the diaphragm, and day 14 in the stomach. The liver of the majority of all animals, mutant and wild-type, contained myelopoietic cells at the earliest days, with myelopoietic cells in the wild-type animals diminishing with age. The epithelial hyperplasia seen in the stomach, pancreas, salivary gland, and liver were never observed in the absence of inflammation, suggesting that they may be a response to inflammation. The ultrastructural differences in cardiomyocytes were seen at or before the first observed inflammatory infiltration, suggesting that aberrant growth control in the heart may be independent of cardiac inflammation.

TGF-β1 thus has a critical regulatory role *in vivo* in the control of the inflammatory response, and the absence of TGF-β1 may have a role in autoimmunity. Because TGF-β1 has such diverse roles, it is difficult to pinpoint the exact mechanisms of the inflammation. Multiple factors may combine to produce the patterns of inflammation seen in these TGF-β1-deficient mice.

Additional studies to define the pathogenesis of the lesions will include transfer of the mutation onto a SCID mouse line to better delineate the role of lymphocytes in the pathogenesis of the multisystemic disease, rederivation as gnotobiotic animals to define the role of bacteria, especially in the digestive system, treatment regimens to inhibit inflammation, and examination of embryos to determine the cause of intrauterine death.

Acknowledgments

We thank Rita Angel and Kathy Bailey for preparation of histology tissues and slides, Frost N. L. Smith for morphometric analysis, and Wen-Yun Sun for genotyping.

References

1. Barnard JA, Lyons RM, Moses HL: The cell biology of transforming growth factor β. Biochim Biophys Acta 1990, 1032:79–87
2. Massague J: The transforming growth factor β family. Annu Rev Cell Biol 1990, 6:597–641
3. Sporn MB, Roberts AB: TGF-β problems and prospects. Cell Regul 1990, 1:875–882
4. Wahl SM: Transforming growth factor β (TGF-β) in inflammation: a cause and a cure. J Clin Immunol 1992, 12:61–74
5. Wallik SC, Figari IS, Morris RE, Levinson AD, Palladino MA: Immunoregulatory role of transforming growth factor β (TGF-β) in development of killer cells: comparison of active and latent TGF-β1. J Exp Med 1990, 172:1777–1784
6. Espevik T, Figari IS, Shalaby MR, Lakides GA, Lewis GD, Shepard HM, Palladino MA: Inhibition of cytokine production by cyclosporin A and transforming growth factor β. J Exp Med 1987, 166:571–576
7. Carlino JA, Higley HR, Creson JR, Avis PA, Ogawa Y, Ellingworth LR: Transforming growth factor β1 systemically modulates granuloid, erythroid, lymphoid, and thrombocytic cells in mice. Exp Hematol 1992, 20: 943–950
8. Kuruvilla AP, Shah R, Hochwald GM, Liggitt HD, Paladino MA, Thorbecke GJ: Protective effect of transforming growth factor β1 on experimental autoimmune diseases in mice. Proc Natl Acad Sci USA 1991, 88: 2918–2921
9. Lalho M, DeCaprio J, Ludlow J, Livingston D, Massague J: Growth inhibition by TGF-β linked to suppression of retinoblastoma protein phosphorylation. Cell 1990, 62:175–185
10. Shull MM, Ormsby I, Kier AB, Pawlowski S, Diebold RJ, Yin M, Allen R, Sidman C, Proetzel G, Calvin D, Annunziata N, Doetschman T: Targeted disruption of the mouse transforming growth factor-β1 gene results in multifocal inflammatory disease. Nature 1992, 359: 693–699
11. Kulkarni AB, Huh C-G, Becker D, Geiser A, Lyght M, Flanders KC, Roberts AB, Sporn MB, Ward JM, Karlsson S: Transforming growth factor β_1 null mutation in

mice causes excessive inflammatory response and early death. Proc Natl Acad Sci USA 1993, 90:770–774

12. Geiser AG, Letterio JJ, Kulkarni AB, Karlsson S, Roberts AB, Sporn MB: Transforming growth factor β_1 (TGFβ_1) controls expression of major histocompatibility antigen expression in the pathogenesis of the TGFβ_1 null mouse phenotype. Proc Natl Acad Sci USA 1993, 90:9944–9948
13. Hines KL, Kulkarni AB, McCarthy JB, Tian H, Ward JM, Chris M, McCartney-Francis NL, Furcht LT, Karlsson S, Wahl SM: Synthetic fibronectin peptides interrupt inflammatory cell infiltration in transforming growth factor β1 knockout mice. Proc Natl Acad Sci USA 1994, 91:5187–5191
14. Tanaka K, Tilney NL, Kupiec-Weglinski JW: Maturing thymocytes in accelerated rejection of cardiac allografts in presensitized rats. Transplantation 1992, 54:515–519
15. Rumyantsev PP: Interrelations of the proliferation and differentiation processes during cardiac myogenesis and regeneration. International Review of Cytology, vol 51. Edited by GH Bourne, JF Danielli, and KW Jeon. New York, Academic Press, 1977, pp 187–277
16. Engelmann GL, Boehm KD, Birchenall-Roberts MC, Ruscetti FW: Transforming growth factor-β_1 in heart development. Mech Dev 1992, 38:85–98
17. Letterio JJ, Geiser AG, Kulkami AB, Roche NS, Sporn MB, Roberts AB: Maternal rescue of transforming growth factor-β1 null mice. Science 1994, 264:1936–1938
18. Zhang J, Yu Z-x, Hilbert SL, Yamaguchi M, Chadwick DP, Herman EH, Ferrans VJ: Cardiotoxicity of human recombinant interleukin-2 in rats: a morphologic study. Circulation 1993, 87:1340–1353
19. Ciacci C, Lind SE, Podolsky DK: Transforming growth factor β regulation of migration in wounded rat intestinal epithelial monolayers. Gastroenterology 1993, 105: 93–101
20. Basson MD, Modlin IM, Flynn SD, Jena BP, Madri JA: Independent modulation of enterocyte migration and proliferation by growth factors, matrix proteins, and pharmacologic agents in an in vitro model of mucosal healing. Surgery 1992, 112:299–308
21. Livingston EH, Guth PH: Peptic ulcer disease. Am Sci 1992, 80:592–598
22. Mezey E, Palkovits M: Localization of targets for antiulcer drugs in cells of the immune system. Science 1992, 258:1662–1665
23. Glick AB, Kulkarni AB, Tennenbaum T, Hennings H, Flanders KC, O'Reilly M, Sporn MB, Karlsson S, Yuspa SH: Loss of expression of transforming growth factor β in skin and skin tumors is associated with hyperproliferation and a high risk for malignant conversion. Proc Natl Acad Sci USA 1993, 90:6075–6080
24. Keller JR, Garwin KS, Ellingsworth LR, Ruscetti FW: Transforming growth factor β: possible roles in the regulation of normal and leukemic hematopoietic cell growth. J Cell Biochem 1989, 39:175–184
25. Hooper WC: The role of transforming growth factor-β in hematopoiesis: a review. Leuk Res 1991, 15:179–184
26. Cotran RS, Kumar V (Eds): Robbins Pathologic Basis of Disease. Philadelphia, WB Saunders Co, 1989, pp 202–204
27. Constantopoulos SH, Tsianos EV, Moutsopoulos HM: Pulmonary and gastrointestinal manifestations of Sjogren's syndrome. Rheum Dis Clin N Am 1992, 18: 617–635